

Rapid Communications

## Aggregation-induced Emission of Non-conjugated Poly(amido amine)s: Discovering, Luminescent Mechanism Understanding and Bioapplication \*

Rui-bin Wang<sup>a, b</sup>, Wang-zhang Yuan<sup>a</sup> and Xin-yuan Zhu<sup>a\*\*</sup>

<sup>a</sup>School of Chemistry and Chemical Engineering, Shanghai Key Lab of Electrical Insulation and Thermal Aging, Shanghai Jiao Tong University, Shanghai 200240, China

<sup>b</sup>Instrumental Analysis Center, Shanghai Jiao Tong University, Shanghai 200240, China

**Abstract** It is found that the fluorescence of aliphatic poly(amido amine)s including linear and hyperbranched ones can be dramatically enhanced by simple aggregation of polymer chains, attributing to the formation of a variety of intra- and interchain clusters with shared lone-pair electrons and the restriction of intramolecular motions. Thanks to the combination of strong solid fluorescence and excellent biocompatibility, these non-conjugated polymers become promising candidates for bioimaging such as bacterial detection. This finding not only extends the aggregation-induced emission (AIE) systems from conjugated compounds to non-conjugated materials, which expands the bioapplication range of AIE systems, but also sheds light on the exploration of novel unconventional luminogens.

**Keywords:** Luminescence; Aggregation-induced emission; Non-conjugated polymer.

**Electronic Supplementary Material** Supplementary material is available in the online version of this article at <http://dx.doi.org/10.1007/s10118-015-1635-x>.

The discovery of aggregation-induced emission (AIE) of conjugated compounds provides an efficient strategy for avoiding the conventional aggregation-caused emission quenching<sup>[1]</sup>. In the past decade, the AIE molecules and polymers have attracted much attention because of their potential applications especially in the biological imaging and detection<sup>[2]</sup>. However, almost all of these AIE molecules and polymers have highly hydrophobic conjugated structure, which brings a lot of troubles for the biological applications, such as poor aqueous solubility, high cytotoxicity, acute inflammation and serious immunogenicity. Therefore, the development of new AIE systems to overcome these shortcomings of conjugates becomes imperative. In recent years, it has been reported that some aliphatic polymers including poly(amido amine) (PAMAM), poly(amino ester), polyethylenimine (PEI) and polypropyleneimine (PPI) can also emit in solutions<sup>[3–6]</sup>. Different from conventional AIE compounds, these polymers have no classic chromophores while exhibiting excellent hydrophilicity and biocompatibility. Unfortunately, the emission of these non-conjugated polymers is usually very weak. Therefore, a tedious polymeric modification has to be performed for the emission enhancement. In the present study, we find that the fluorescence of aliphatic PAMAMs including linear and hyperbranched ones can be dramatically enhanced by simple aggregation of polymer chains, thus extending the AIE systems into non-conjugated materials. Ascribed to the perfect combination of strong fluorescence and excellent biocompatibility, these non-conjugated polymers will greatly expand the application range of AIE systems in

\* This work was financially supported by the National Basic Research Program (No. 2015CB931801), and the National Natural Science Foundation of China (Nos. 21204049 and 51473093).

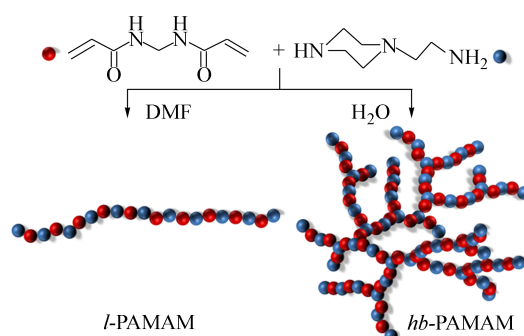
\*\* Corresponding author: Xin-yuan Zhu (朱新远), E-mail: xyzhu@sjtu.edu.cn

Received February 11, 2015; Accepted February 13, 2015

doi: 10.1007/s10118-015-1635-x

biological fields. Moreover, the emission mechanism understanding of these non-conjugated systems will surely shed light on the development of novel luminescent materials.

Non-conjugated linear (*l*) and hyperbranched (*hb*) PAMAMs were synthesized by Michael-type polycondensation-addition of *N,N'*-methylene bisacrylamide (MBA) and 1-(2-aminoethyl)piperazine (AP) with an equal feeding mole ratio at 60 °C<sup>[7]</sup>, as illustrated in Scheme 1 and Chart S1 in the Supporting Information. The polymerized products were fully characterized by NMR, IR, DSC and GPC-MALLS, with satisfactory results obtained (Chart S2 and Figs. S1–S5 in Supporting Information). Based on the NMR analysis, different topological structures of PAMAMs were confirmed. *l*-PAMAM [degree of branching (DB) = 0] was formed when the polymerization was carried out in *N,N'*-dimethylformamide (DMF), whereas *hb*-PAMAM with DB of 0.44 was obtained if the solvent was replaced by water. Table 1 summarizes the weight average molecular weight ( $M_w$ ) and molecular weight distribution ( $M_w/M_n$ ), DB, glass transition temperature ( $T_g$ ) of both polymers. Notably, with comparable or even higher  $M_w$  (8480) and narrower  $M_w/M_n$  (1.3) compared to those of *l*-PAMAM ( $M_w = 8030$ ,  $M_w/M_n = 1.8$ ), *hb*-PAMAM exhibits much lower  $T_g$  of 11.3 °C than that of *l*-PAMAM (18.9 °C), which should be ascribed to its hyperbranched structure and thus looser packing and weaker intra- and intermolecular interactions in the solid state.



**Scheme 1** Synthetic route to linear (*l*) and hyperbranched (*hb*) PAMAMs

**Table 1.** Characterization data of *l*-PAMAM and *hb*-PAMAM

Sample	DB <sup>b</sup>	$M_w$	$M_w/M_n$	$T_g$ <sup>c</sup> (°C)	$\Phi_{F,f}$ <sup>d</sup> (%)	$\Phi_{F,s}$ <sup>d,e</sup> (%)
<i>l</i> -PAMAM	0	8 030	1.8	18.9	14.9	0
<i>hb</i> -PAMAM	0.44	8 480	1.3	11.3	5.2	0

<sup>a</sup> The feeding mole ratio of MBA to AP was 1:1; The reaction was carried out at 60 °C for 60 h; <sup>b</sup> Calculated from quantitative <sup>13</sup>C-NMR results by Equation S1; <sup>c</sup> Determined by DSC; <sup>d</sup>  $\Phi_{F,f}$  and  $\Phi_{F,s}$  are the quantum yields of the film and solution, respectively; <sup>e</sup> Concentration = 10 µg/mL

Both linear and hyperbranched PAMAMs show good solubility in aqueous solution while being insoluble in acetone. When the dilute aqueous solutions of PAMAMs are excited at 380 nm, no visible photoluminescence (PL) is observed, with rather low emission signals being recorded (Fig. 1). Interestingly, both the absorption intensity at 380 nm and the PL intensity at 450 nm increase almost linearly with the concentration of PAMAMs in a wide range (Figs. 2a, 2b and Fig. S6 in Supporting Information); meanwhile, the emission of PAMAMs has been progressively lighted up with increased concentration (Fig. 2c). Since polymer chains readily collapse and aggregate at high concentrations, the above results indicate the AIE feature of PAMAMs. Comparing to those of *hb*-PAMAM, the absorption and emission intensities of *l*-PAMAM grow more quickly, which might be ascribed to its more compactly aggregated structure. To further confirm the AIE nature of the polymers, a large amount of acetone was added into their aqueous solutions. Acetone was chosen because it is a typical nonsolvent for PAMAMs: the polymer chains must aggregate in the aqueous mixtures with massive acetone, as verified by the cloudy pictures in Fig. S7 of Supporting Information. As depicted in Fig. 1, in the 5/95 water/acetone mixture, the PL intensities are significantly enhanced, giving bright blue emissions with maxima at ~455 and 441 nm for *l*-PAMAM and *hb*-PAMAM, respectively.

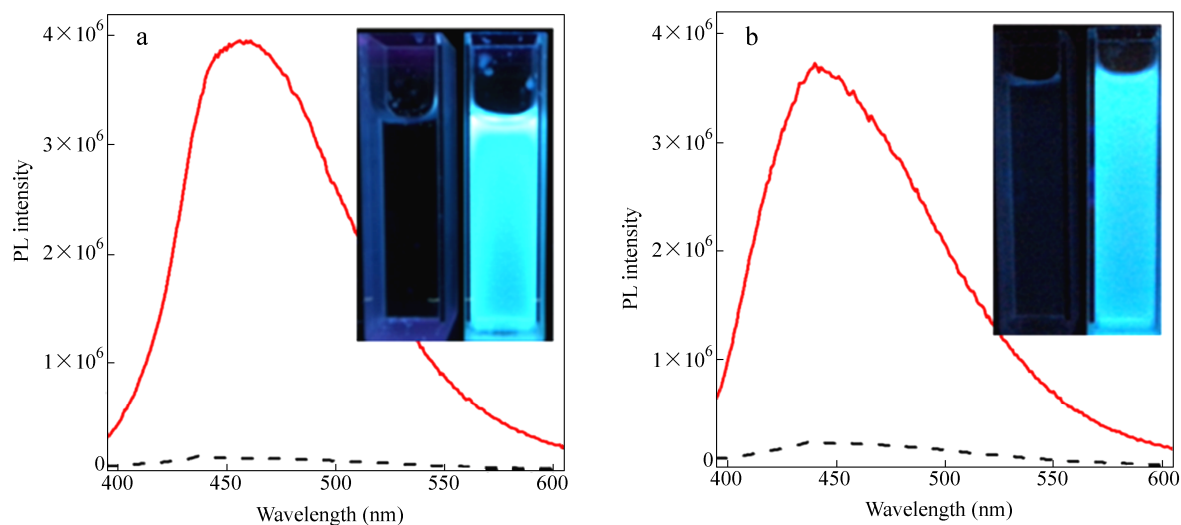


**Fig. 1** Emission spectra of (a) *l*-PAMAM and (b) *hb*-PAMAM in dilute aqueous solution (dash) and in 5/95 (*V/V*) water/acetone mixture (solid) Concentration = 10  $\mu\text{g/mL}$ , excitation wavelength = 380 nm. Inset: the photographs of PAMAMs in water (left) and 5/95 (*V/V*) water/acetone (right) mixture taken under 365 nm UV light irradiation.

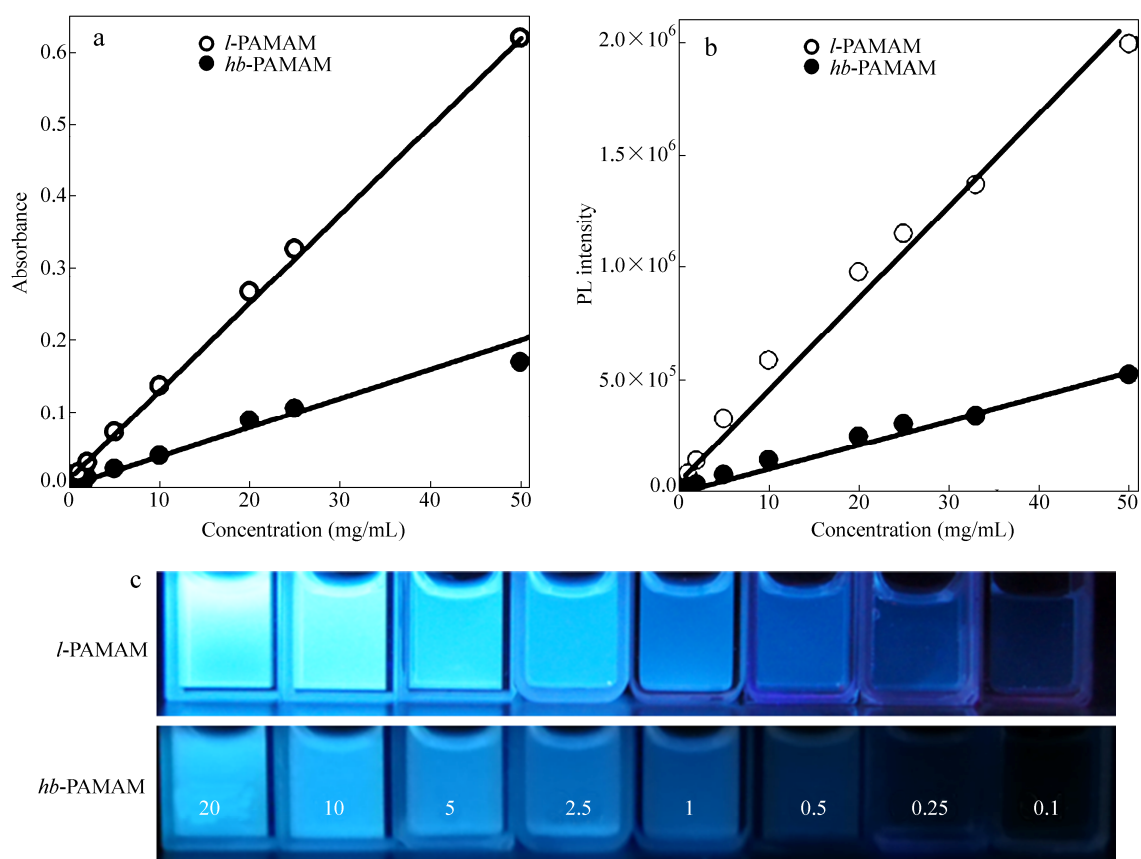


**Fig. 2** (a) Absorption intensity (at 380 nm), (b) emission intensity (at 450 nm) and (c) photographs (taken under 365 nm UV light) of aqueous solutions of *l*-PAMAM and *hb*-PAMAM at different concentrations (mg/mL) as indicated (For (b), excitation wavelength = 380 nm)

Solid films of linear and hyperbranched PAMAMs on the quartz plates (Fig. S8 in Supporting Information) also emit intensively. Interestingly, the PL spectra of PAMAM films are red shifted with increasing excitation wavelength. For example, the emission peaks of *l*-PAMAM/*hb*-PAMAM are bathochromically shifted from ~471/463 to 512/534 and then to 558/570 nm as the excitation wavelength increases from 380 to 460 and then to 530 nm (Fig. 3). The excitation wavelength dependent emission of PAMAM films clearly suggests the presence of varying emission species, which are sensitive to varied excitations. This is further verified by the time-resolved PL measurement, from which different lifetimes are obtained at varying monitoring wavelengths (Fig. S9 in Supporting Information).

Besides efficient emission, high photostability is also extremely desirable for the luminogens. For the polymeric thin films, when observed under fluorescence microscope upon excitations by UV, blue and green lights, bright and stable fluorescences with blue, green and red colors are observed (Fig. 3). After a long period of excitation, little emission difference is detected between the first and the 100th scans with total irradiation time of ~10 min (Video S1–S6 in Supporting Information), thus suggesting the excellent photostability of the films.

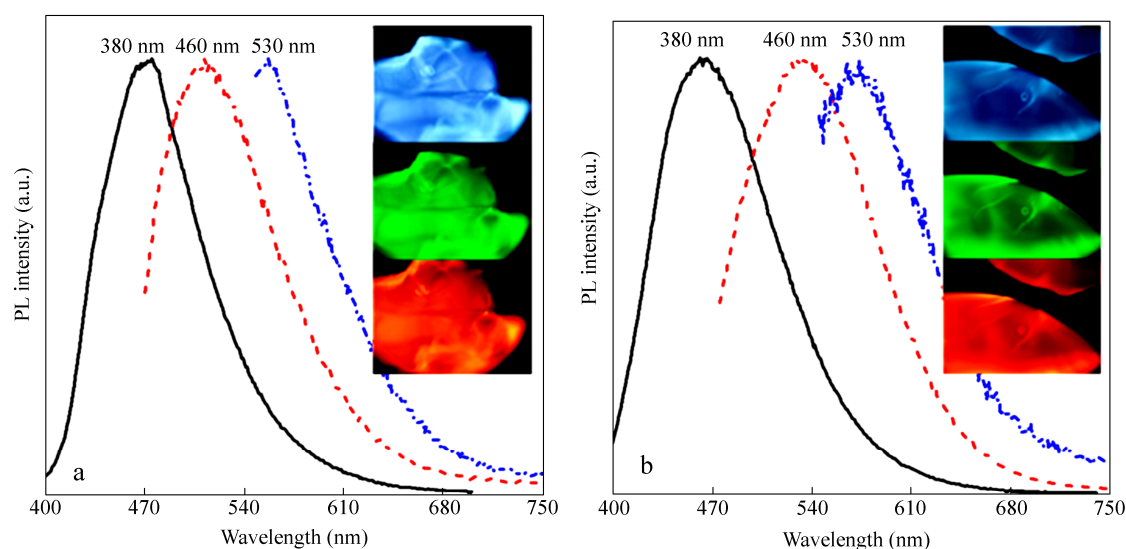


**Fig. 3** Emission spectra of (a) *l*-PAMAM and (b) *hb*-PAMAM solid films at different excitation wavelengths as indicated; Inset: fluorescence images of PAMAM solid films taken under illumination of UV (top), blue (media) and green (bottom) lights

To quantitatively evaluate the emission property of PAMAMs, their absolute PL quantum yields in the solution ( $\Phi_{F,s}$ ) and film ( $\Phi_{F,f}$ ) states were determined by an integrating sphere<sup>[8]</sup>, and the results are listed in Table 1. For the aqueous solutions at a concentration of 10  $\mu\text{g/mL}$ , no valuable emission signals were recorded, giving  $\Phi_{F,s}$  values of nought. Their  $\Phi_{F,f}$  values, however, are boosted to 14.9% and 5.2% for *l*-PAMAM and *hb*-PAMAM films, respectively, demonstrating remarkable AIE effect. The higher quantum yield of the former might be related to its tight molecular stacking and stronger molecular interactions, as supported by the  $T_g$  result.

All above results definitely suggest the AIE characteristics of PAMAMs, regardless of their polymer architecture. As a kind of non-conjugated polymers, PAMAMs have no conventional chromophores, it is thus of crucial importance to decipher the origin of the emission. Despite there is no classic chromophore, there are a large number of amide and amine groups with lone-pair electrons. In order to better understand the emission mechanism, theoretical calculation of a simplified PAMAM fragment with two repeating units was carried out by using Gaussian 09 based on density functional theory (DFT) at the RB3LYP/6-31G+ (d) level. It is found that the isolated and periodic lone-pair electrons and delocalized  $\pi$  electrons in the polymer chain can form a variety



of intra- and interchain clusters (Fig. 4). Instead of the interaction by thermodynamically controlled random approaching, these lone-pair electrons and  $\pi$  electrons can further delocalize through n- $\pi$  and  $\pi$ - $\pi$  interactions in the aggregates. In comparison with isolated groups, such clusters with shared and overlapped electron clouds exhibit smaller energy gaps and extended electronic conjugations. Moreover, upon aggregation, nonradiative deactivation pathways of the excitons are impeded due to the rigidified conformations resulting from effective intra- and intermolecular interactions, thereby making such “cluster chromophores” highly emissive. Accordingly, the excitation wavelength dependent emissions of the aggregates and solid films should be attributed to the heterogeneity of the clusters.

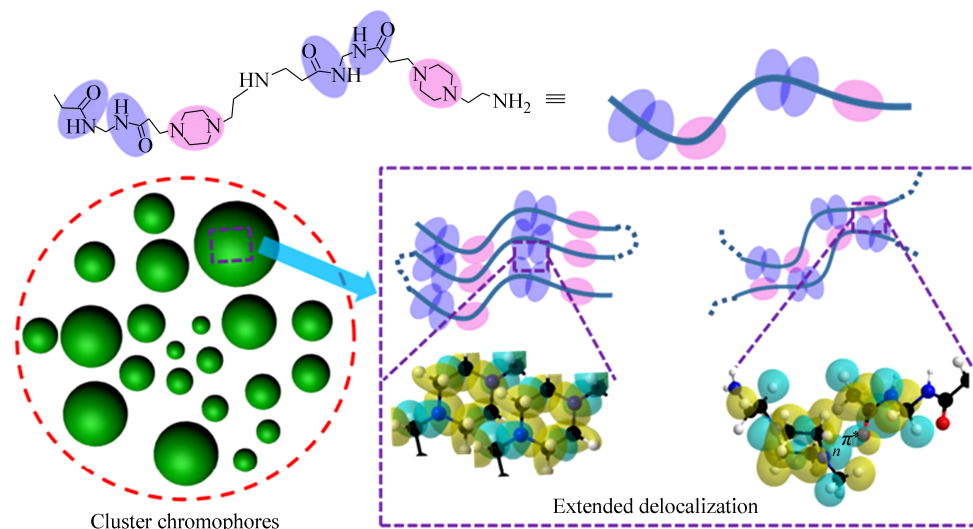


**Fig. 4** Schematic illustration of the emission mechanism of PAMAMs based on the calculation

Tang and Virgili have identified restriction of intramolecular rotation (RIR) in the aggregates as the main cause for the general AIE systems<sup>[9, 10]</sup>. For PAMAMs, based on the above results, their AIE phenomenon is understandable: when molecularly dispersed, they are non-emissive, owing to the lack of suitable chromophores with extended conjugation and the effective quenching by molecular motions; upon aggregation, “cluster chromophores” with extended electronic delocalization are formed, and conformation rigidification renders them highly luminescent.

To gain further insights into the AIE behavior of PAMAMs, the temperature effect on the emission of PAMAM films was investigated. Figure 5 shows that the PL intensity of linear and hyperbranched PAMAM films increases almost linearly with decreasing temperature when they are cooled from 80 °C to 20 °C, indicating that the thermally activated intramolecular motions (vibrations and rotations) are gradually impeded during cooling. Afterwards, sharp increases in the PL peak intensity are monitored with continuously decreased temperature from 20 °C to 0 °C, giving the inflection points of 19.5 and 11.8 °C for *l*-PAMAM and *hb*-PAMAM, respectively, which are approaching to their  $T_g$  values obtained from DSC measurement. These results are reasonable that the freezing of polymer segments remarkably contributes to the reduction of nonradiative deactivation of the excitons, thus boosting the emissions. The peak intensity of both polymers, however, clearly levels off at further lowered temperatures, suggesting limited impact of further cooling. This observation also confirms the essential role of structural rigidification of “cluster chromophores” for the AIE phenomenon of non-conjugated PAMAMs.

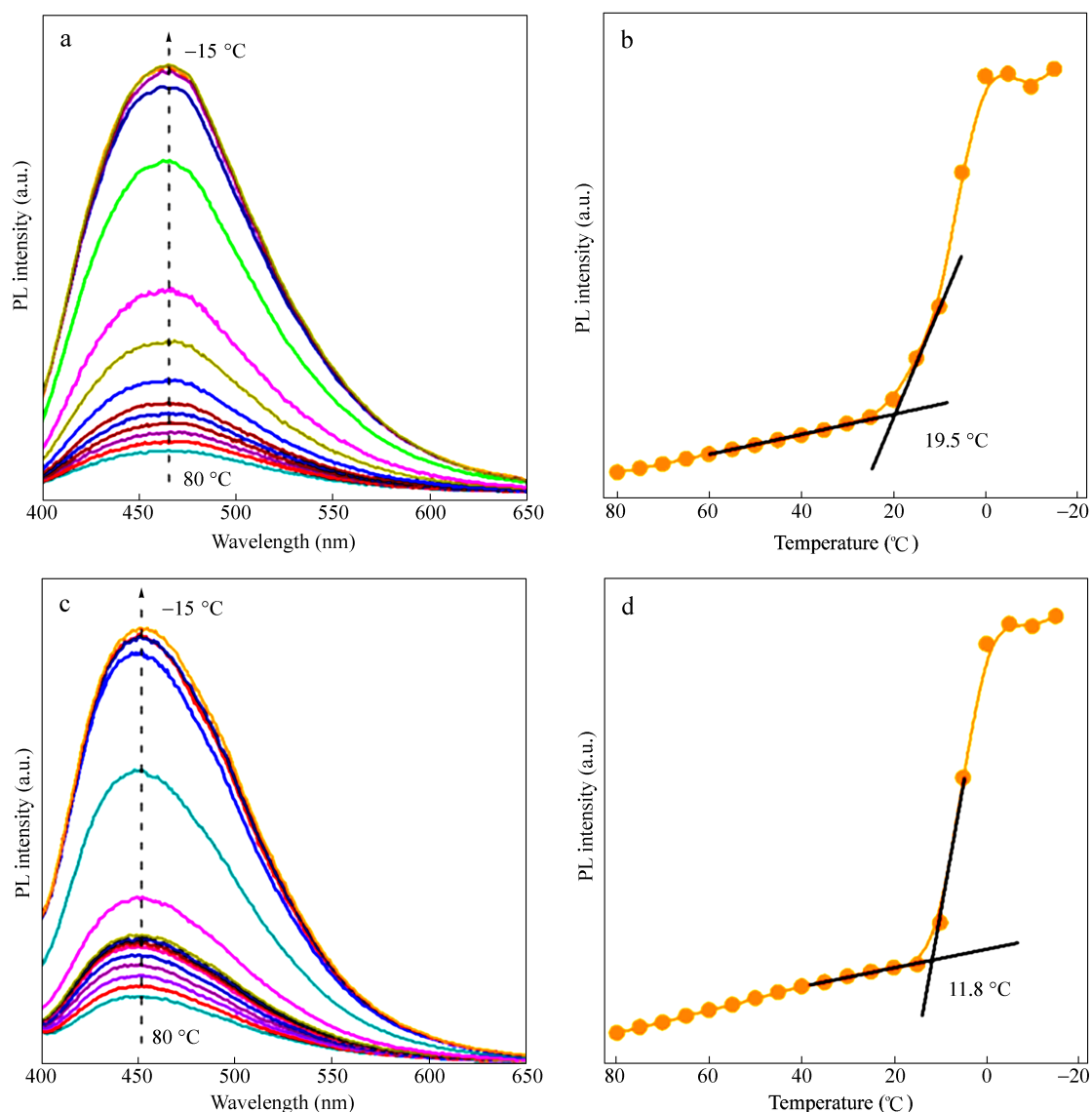


**Fig. 5** (a, c) Emission spectra and (b, d) peak intensities of *l*-PAMAM (a, b) and *hb*-PAMAM (c, d) at varying temperatures (Excitation wavelength = 380 nm)

The cytotoxicity of linear and hyperbranched PAMAMs in comparison with PEI (25 kDa) was evaluated using the MTT assay in COS-7 cell line after 48 h incubation with polymers. As shown in Fig. S10 in Supporting Information, *hb*-PAMAM exhibits less toxicity in COS-7 cells than *l*-PAMAM. Moreover, the cytotoxicity of both samples is much lower than that of the PEI control, which is the mostly used agent for drug and gene delivery. The low cytotoxicity and AIE feature of PAMAMs prompted us to further investigate their performance in biological imaging. PAMAM molecules are positively charged because of the presence of numerous primary, secondary and/or tertiary amines in the polymer chains, which are suitable for binding to such anionic biomembranes as bacteria and cells through electrostatic interactions<sup>[11]</sup>. As an example, we clarified that these AIE-active PAMAMs can be used as a powerful tool for the detection of bacteria. After incubating 4 mL of *E. coli* suspension (optical density of the sample at 600 nm ( $OD_{600}$ ) is 1.0) with 500  $\mu$ L of PAMAMs (1 mg/mL in PBS) for 15 min, the aggregates of *E. coli* were centrifuged and detected by fluorescence microscope. As demonstrated in Fig. 6, in the solution state, the fluorescent images of PAMAM/*E. coli*

complexes show very weak blue fluorescence (Figs. 6a, 6b), and almost no green and red fluorescence can be observed (Figs. S11, S12 in Supporting Information). After freeze-drying, bright blue (Figs. 6c, 6d), green and red emission (Figs. S11, S12 in Supporting Information) of *E. coli* clusters are clearly observed. Such strong fluorescence should be attributed to the emission of aggregated PAMAMs rather than *E. coli*, because pure *E. coli* is identified as nonluminescent (Fig. S13 in Supporting Information). These results indicate that PAMAMs have successfully bound to *E. coli* clusters. After freeze-drying, the AIE feature of PAMAM/*E. coli* aggregates greatly improves the detection sensitivity of bacteria, allowing the detection limit as low as  $10^2$  cfu/mL (Figs. S14, S15 in Supporting Information).

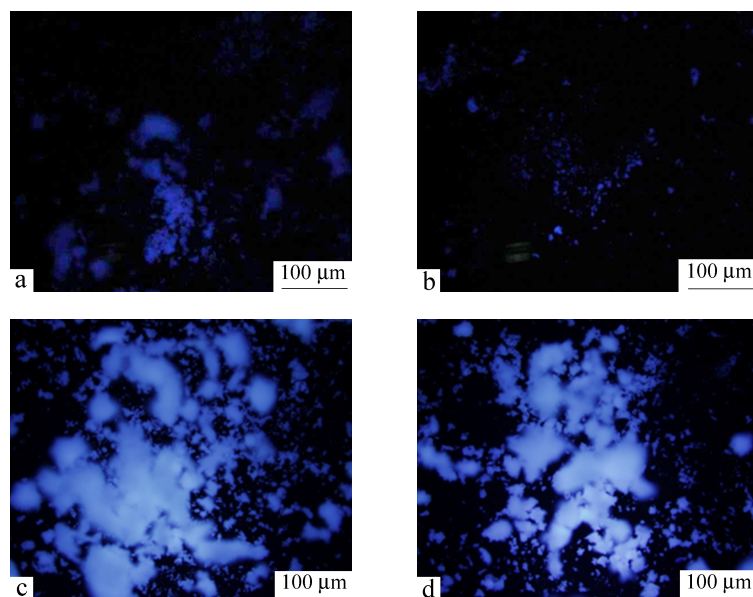


**Fig. 6** Fluorescence microscope images of (a, c) *l*-PAMAM/*E. coli* and (b, d) *hb*-PAMAM/*E. coli* aggregates before (a, b) and after (c, d) freeze-drying (Excitation wavelength = 380 nm)

In summary, we find that the fluorescence of non-conjugated PAMAMs including linear and hyperbranched ones can be dramatically enhanced by the aggregation of polymer chains, which extends the AIE systems from conjugated compounds to non-conjugated materials. The emission mechanism of these luminogens without classic chromophores is ascribed to the formation of varying clusters consisting of amide and amine groups with lone-pair electrons. The AIE mechanism is attributed to the structural rigidification of these “cluster chromophores” resulting from the restriction of intramolecular motions (vibration and rotation). Unlike general conjugated AIE molecules and polymers, PAMAMs take advantages of excellent hydrophilicity and good biocompatibility. Together with their efficient emission in the aggregated states, they are promising for biological imaging such as bacterial detection. Further studies on the development of novel non-conjugated AIE materials and their biomedical applications are underway in our laboratory.

## REFERENCES

- 1 Luo, J., Xie, Z., Lam, J.W.Y., Cheng, L., Chen, H., Qiu, C., Kwok, H.S., Zhan, X., Liu, Y., Zhu, D. and Tang, B.Z., *Chem. Commun.*, 2001, 18: 1740
- 2 Hong, Y., Lam, J.W.Y. and Tang, B.Z., *Chem. Soc. Rev.*, 2011, 40: 5361
- 3 Lee, W.I., Bae, Y.J. and Bard, A.J., *J. Am. Chem. Soc.*, 2004, 126: 8358
- 4 Wang, D.J. and Imae, T., *J. Am. Chem. Soc.*, 2004, 126: 13204

- 5 Wu, D.C., Liu, Y., He, C.B. and Goh, S.H., *Macromolecules*, 2005, 38: 9906
- 6 Sun, M., Hong, C.Y. and Pan, C.Y., *J. Am. Chem. Soc.*, 2012, 134: 20581
- 7 Wang, R.B., Zhou, L.Z., Zhou, Y.F., Li, G.L., Zhu, X.Y., Gu, H.C., Jiang, X.L., Li, H.Q., Wu, J.L., He, L., Guo, X.Q., Zhu, B.S. and Yan, D.Y., *Biomacromolecules*, 2010, 11: 489
- 8 Porrès, L., Holland, A., Pålsson, L.-O., Monkman, A.P., Kemp, C. and Beeby, A., *J. Fluoresc.*, 2006, 16: 267
- 9 Chen, J., Law, C.C.W., Lam, J.W.Y., Dong, Y., Lo, S.M.F., Williams, I.D., Zhu, D. and Tang, B.Z., *Chem. Mater.*, 2003, 15: 1535
- 10 Virgili, T., Forni, A., Cariati, E., Pasini, D. and Botta, C., *J. Phys. Chem. C*, 2013, 117: 27161
- 11 Yang, W., Pan, C.Y., Luo, M.D. and Zhang, H.B., *Biomacromolecules*, 2010, 11: 1840